Journal of Materials Chemistry A

Accepted Manuscript

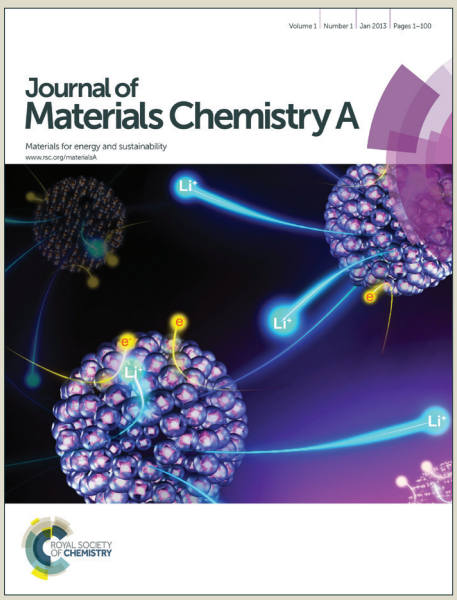

ROYAL SOCIETY OF CHEMISTRY

www.rsc.org/materialsA

Graphene oxide modified polyamide nanofiltration membrane with improved flux and antifouling properties

Saira Bano[1,2,] Asif Mahmood[1,2] Seong-Joong Kim[1], Kew-Ho Lee[1,2,*]

[1]Korea Research Institute of Chemical Technology, Daejeon 305-606, Republic of Korea
[2]Korea University of Science & Technology, Daejeon 305-350, Republic of Korea

ABSTRACT:

Organic-inorganic hybrid materials are considered the most promising candidates in preparation of nanofiltration (NF) membranes. Incorporation of nano-particles in a polymer matrix have provided a new approach for preparation of membranes with enhanced permeability, high selectivity and improved anti-fouling properties. In this study, polyamide (PA) nanofiltration (NF) membranes embedded with various graphene oxide (GO) content to improve the membrane flux and anti-fouling properties are proposed and successfully prepared for desalination applications. The prepared PA/GO membranes exhibited much higher flux than did pristine PA membranes. A twelve-fold increase in water flux, with a negligible change in salt rejection, was observed after incorporating GO (0.2 wt%) in the PA membrane. Addition of GO also provided a significant improvement in the anti-fouling property of the membrane due to an increase in the hydrophilicity of the membrane. These results indicate that incorporation of GO into a PA membrane can effectively enhance its hydrophilicity and consequently improve its flux and antifouling properties. Because no deleterious effect on the performance of the PA membrane was observed from this modification, this concept provides an effective way to develop high performance NF membranes with greater stability.

Introduction

Graphene oxide is a one-atom-thick carbon wafer and has been hyped in recent years as a super material. It has gained much interest in the field of material research owing to its spectacular electrical and mechanical properties.[1–3] Very recently, the eccentric permeability of graphene oxide membrane for water was described, [4,5] which opened a new horizon for its application in water desalination and pervaporation separation of water-organic mixtures.[6–13] Pure GO membranes prepared by solution filtration are unsuitable for water separation because of their instability under extremely hydrophilic conditions. Additionally, pure GO membranes are easily damaged and detached from their support when exposed to the high trans-membrane pressure in NF. Therefore, stable bonding between the GO nano-sheets must be created, or the GO must be blended with

a suitable polymer to overcome this problem.[9] The appropriate blending of the atomically thin GO into a polymer matrix, can significantly improve the physical properties of the host polymers at extremely low doping concentrations.[6–11] In particular, the oxygen-containing functional groups in graphene oxide offer enormous potential for making functional nano-composite (NC) materials with superior chemical stability, strong hydrophilicity, and excellent antifouling properties, compared to the neat polymer. [1–3]

On the other hand, the thin-film composite (TFC) polyamide membranes are widely used for the production of ultrapure water in reverse osmosis and nanofiltration processes.[14,15] The major problem associated with these membranes (fouling) restricts their application for water purification technology.[16-19] Additionally, these membranes have the drawback of low water flux and low energy efficiency.[20, 22] The vulnerability of PA membranes to fouling is mainly related to the hydrophobicity of the polyamide active layer. Though periodic cleaning of membranes is a routine practice used to reduce fouling, it does not solve the problem completely, and the membrane eventually has to be replaced.[23] Much effort has been devoted to improving the flux and anti-fouling properties of PA membranes but surface modification with hydrophilic, low-fouling material is one of the best ways to tune the characteristics of the membrane.[19, 23–27] Recently, the development of a new approach involving incorporation of nanoparticles have resulted in the preparation of membranes with enhanced permeability, high selectivity and good anti-fouling properties.[28, 29] A variety of nano-materials (e.g., metal oxide, Zeolite, carbon nano-tubes, C60 fullerenes, and graphene oxide) can be used to modify PA membranes.[30–39] However, few research studies have involved the use of GO in nanofiltration membranes for desalination.[9,11]

Here, we report novel GO-incorporated PA membranes prepared by interfacial polymerization. To the best of our knowledge, this is the first attempt to use GO for interfacial polymerization. The high water flux of the GO, in combination with the high rejection characteristics of polyamide membrane, leads to an NF membrane of exceptionally high performance. Moreover, the incorporation of GO not only results in increased water flux, but also enhances the antifouling properties of the PA membrane.

Experimental Section

2.1 Materials and reagents

Graphene oxide was manufactured by using graphite flakes purchased from Sigma Aldrich. Analytical grade sodium nitrate ($NaNO_3$), potassium permanganate ($KMnO_4$) and concentrated sulfuric acid (H_2SO_4) (98 wt.%) were obtained from the Samchin Chemical Company, Korea. Polysulfone (Psf) UF Membrane was supplied by the WoongJin Chemical company, Korea. The membranes were used as support for interfacial polymerization. 1,3-phenylene diamine (MPD) was purchased from DuPont. 1,3,5-Benzenetricarbonyl trichloride (TMC), triethylamine (TEA), 2-ethyl-1,3-hexane diol (EHD), camphorsulfonic acid (CSA), dimethylsulfoxide (DMSO), tributyl phosphate (TBP), were purchased from Sigma Aldrich used as additives. Isoparaffin (ISOL-C) was provided by SK Chemical in Korea. All chemicals were used as received. The deion-

ized (DI) water used here was produced with a Milli-Q system (Millipore).All of the reagents and chemicals were of analytical grade and used without further purification. Bovine serum albumin (BSA, MW=67,000).

2.2. Preparation of polyamide / graphene oxide (GO) composite membrane

In this work, Graphene oxide was prepared from graphite using the modified Hummers method.[40,41] Polyamide membranes were prepared by interfacial polymerization on a Psf UF membrane as described previously.[51] The Psf membrane was dipped into an aqueous solution containing MPD/GO and MPD/GO with additives [(TEA (2-3 wt.%), DMSO (1 wt.%), EHD (0.2-0.3 wt.%), and CSA (1-2 wt.%)] in DI water, after which the excess solution was removed by squeezing with a soft rubbery roller after 1 min. The Psf membrane was then immersed in a solution of 0.1 wt.% TMC and 0.3 wt.% TBP in isoparaffin. After 1 min of reaction, the membrane was dried in oven at 60 ^{o}C for 10 minutes. The membrane was put in a 2000ppm Na_2CO_3 solution for 2 minutes. In order to check the effect of GO different wt.% (0.1-0.3 wt.%) were added in aqueous solution. The types of membrane preparations were designated as PA and GO/PA (without additives), or as PA-A and PA-A/GO (with additives) Fig. 1 exhibit formation of PA/GO TFN membrane via interfacial polymerization.

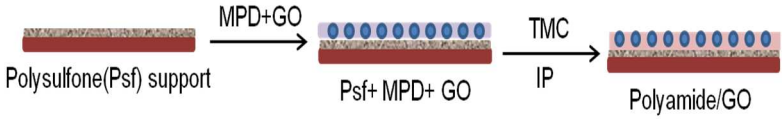

Figure 1 Conceptual illustration of PA/GO nanocomposite membranes

2.3. Membrane characterization

Fourier transform infrared spectroscopy (FT-IR, Perkin-Elmer-283B) was used to detect chemical compositions of the GO and membrane surface. The surface and cross-section morphologies of the membranes were observed with a scanning electron microscope (SEM Tescan Mira 3 LMU FEG) and transmission electron microscope (TEM Tecnai, G2T-20S, 2004). The effect of GO loading on surface roughness was studied by analyzing the membrane surface topology using atomic force microscopy (AFM Seiko, SPA 400, SPI 3800N) technique. The surface hydrophilic behavior of the membrane surface was measured using the water contact angle measurement. To minimize experimental errors, an average value for the contact angle of each membrane was obtained using five measurements.

2.4. Membrane performance testing

Membrane permeation performance was measured with nanofiltration cell. The membrane effective area was 19.6 cm^2, and the permeation test was conducted at 15 °C and 15 bar. Prior to the permeation testing, each membrane was first compacted at 15 bar with feed solution for 20 minutes to obtain a steady flux. The Flux was calculated by using following equation1:

$$J = \frac{V}{S \times t} \qquad (1)$$

Where J is the flux (L.m^{-2}.h^{-1}), V is the permeate volume (L), S is the membrane area (m^2), and t is the time (h). The solute rejection percentage was calculated using the following equation 2,

$$\text{Salt Rejection (\%)} = \left(1 - \frac{C_p}{C_f}\right) \text{x } 100 \qquad (2)$$

Where, C_p and C_f are concentration of permeate and feed solution respectively.

2.5. Antifouling testing

The antifouling property of membranes was measured by using two standard reagents as foulant. A 200ppm BSA solution and 200ppm humic acid with 20ppm calcium chloride was used as the model fouling characteristics of original PA and GO-modified PA membranes. The flux is calculated with variation of time.

Results and Discussion

The interaction of GO with polyamide polymer was confirmed by attenuated total reflectance Fourier transform infrared (ATR FT-IR) spectra (Fig. 2).

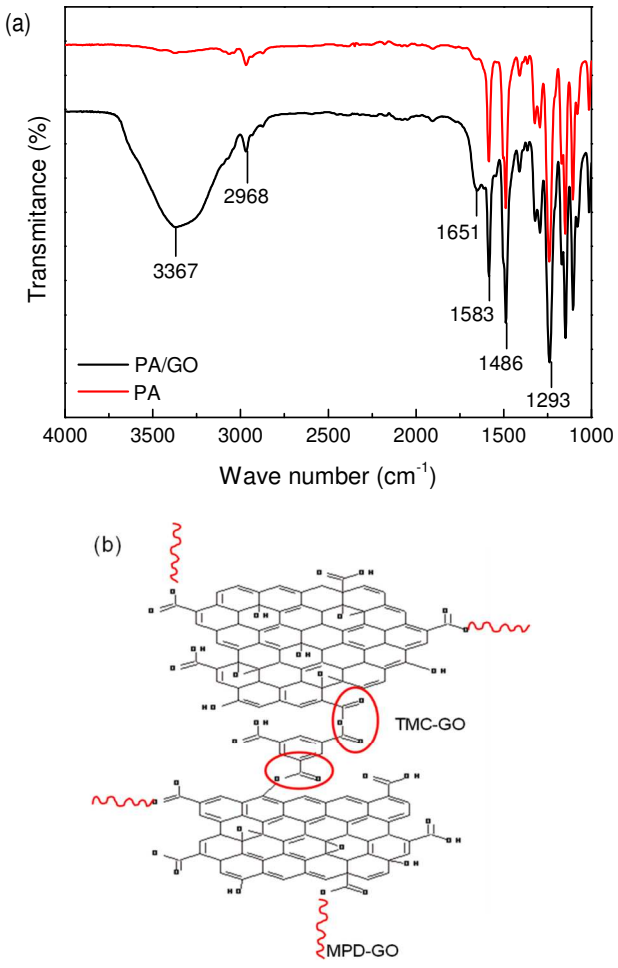

Figure 2 a) FTIR Spectra of PA TFC and PA/GO TFN 2 composite membrane b) Interaction of GO with TMC and MPD

Fig. 2a shows a comparison of the PA and GO modified PA membranes. The most distinctive features of the IR spectra of polyamides are the bands associated with amide linkages. These bands (amide-I and amide-II) are characteristic of amides and appeared at fixed positions with strong intensities.[25, 38] The prominent peak at 1,651 cm^{-1} is due to the carbonyl stretching, vibration, whereas, the amide II band that appears at 1,583-cm^{-1} is chiefly due to couplings of in-plane N-H bending and C-N stretching vibrations of the amide group.[25] Fig. 2a shows an enhancement in absorbance at 1,651 cm^{-1} for the PA/GO membranes, which confirms the reaction of the -COOH group of GO and -NH_2 group of MPD to form some new amide linkages. When GO was introduced into MPD aqueous solution then some of the OH and COOH groups present in GO would be expected to react with MPD to form the amide linkages and thus be incorporated into the polyamide structure during interfacial polymerization.[44] In comparison with the pure PA membrane, the GO modified PA membranes showed an intense and wider absorption band at 3,367 cm^{-1}, which confirms that the surface hydrophilicity is obviously improved.[42,43] The considerable increase in the hydrophilicity of GO-modified PA membrane was also confirmed by the contact angle measurement.

TFC membranes were relatively hydrophobic [12] with a higher contact angle. Table 1 shows that the contact angle decreased with increasing GO content and that this resulted in an increase in the hydrophilicity. The presence of oxygen-containing functional groups in GO are thought to improve the hydrophilicity of the membrane, which in turn would result in greater water flux.[8, 11, 42–43, 45]

Table 1 Contact angle and root mean surface roughness (RMS), root average arithmetic roughness (R_a), and root peak-to-valley (R_{pv}) values of the TFC and TFN membranes

Sample	GO	Roughness [nm]			Contact angle
	[%]	RMS	R_a	R_{pv}	[°]
TFC	0.0	69.88	56.50	435.70	88±3
TFN 1	0.1	43.35	35.56	335.73	66±2
TFN 2	0.2	34.42	26.00	245.73	65±3
TFN 3	0.3	22.49	16.38	174.41	60±1

The surface properties of the membrane were further investigated using the zeta potential. Fig. 3 shows that the addition of GO to the PA membrane not only decreased its contact angle, but also induced a surface negative charge. Furthermore, at higher pH, membrane with high GO content, exhibited a more negative surface charge because of the presence of more carboxylic groups and their deprotonation, respectively. [46, 47]

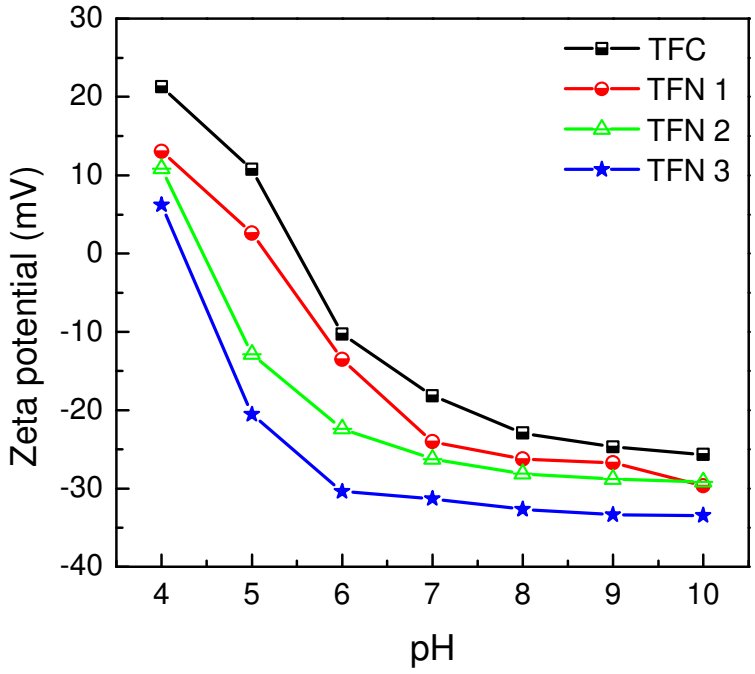

Figure 3 Surface charge vs GO contents over pH range

The surface morphology and surface roughness of the membrane were analyzed using scanning electron microscopy (SEM) and atomic force microscopy (AFM). The SEM and AFM images of the top surface of thin-film composite (TFC/PA) and thin-film nanocomposite (TFN/PA/GO) membranes are shown in Fig. 4, parts a–d. Both TFC and TFN membranes had a rough and leaf like structure on their surfaces that is a peculiar feature of the PA membrane surface.[30–35] However, the TFN membrane (Fig. 4b and 4d) has a denser structure throughout the plane as compared to the TFC membrane with its nodular surface. This is because the formation of the polyamide layer over the support layer depends on the reaction rate during interfacial polymerization, and on hydrogen bonding. The membrane surface morphology greatly changed after addition of GO-containing hydroxyl and carboxyl groups.

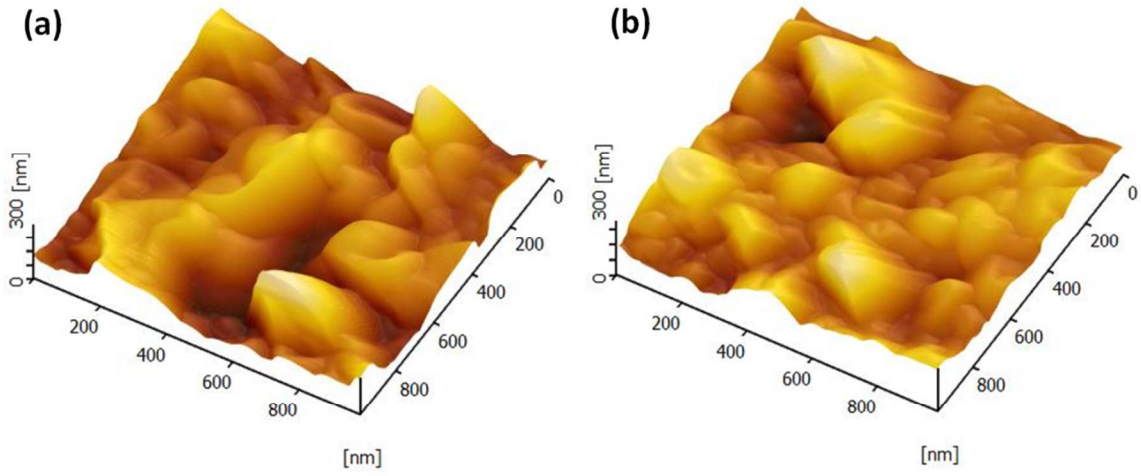

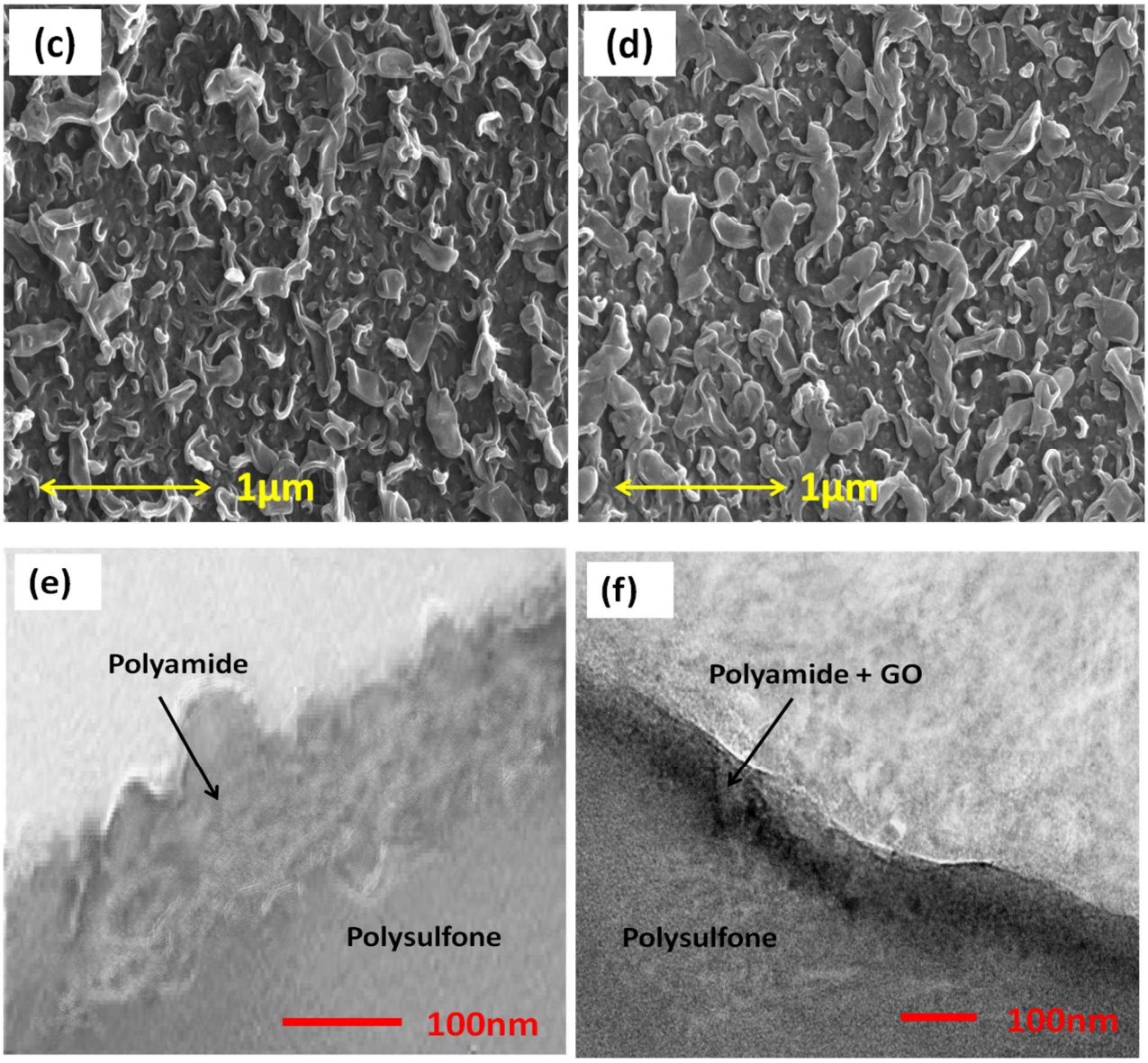

Figure 4 AFM, SEM and TEM images of polyamide TFC (a, c,e) and TFN 2 (b, d,f) membranes

The denser surface in Fig. 4d may be attributed to the carboxyl groups grafted onto the GO surface. The slow reaction of TMC with the GO-carboxyl groups resulted in a leaf-like surface. In contrast, the fast reaction of MPD with TMC during interfacial polymerization resulted in a nodular structure. Additionally, the hydroxyl groups present on GO underwent hydrogen bonding, resulting in a more compact chain structure. Similar results have been reported for carbon-nanotube modified PA membranes.[55] On the other hand, three-dimensional AFM images of thin-film composite membranes, with and without GO, exhibited the characteristic "ridge-and-valley" structure of polyamide, distributed throughout the plane. The root mean square roughness (RMS), root average arithmetic roughness (R_a) and root peak-to-valley distance (R_{pv}) of the membrane surface is listed in Table 1. The incorporation of GO into the TFN polyamide matrix (Fig. 4b) somehow creates more variable and broader ridges. This observation agrees with the SEM images wherein the TFN mem-

branes generated more obvious "leaf-like" folds, which correspond to the ridges seen in AFM. Transmission electron microscope images of pure PA and PA/GO are presented in Fig. 4e, f. PA membrane exhibits nanoscale roughness in x-section that is the particular property of TFC membrane, while on the other hand PA/GO membrane possesses relatively smooth surface with GO apparently visible in cross section of TFN. The PA/GO surface smoothness is also evident from AFM images. Both of the membranes have an active layer thickness in 50-200nm range.[34]

To investigate the effect of GO on the permeance properties of a GO/PA membrane, TFN membranes with different GO concentrations were prepared and tested in an NF experiment. Fig. 5 shows that the flux increases with increasing the GO content (up to 0.2%) and then starts decreasing. (Fig. 5)

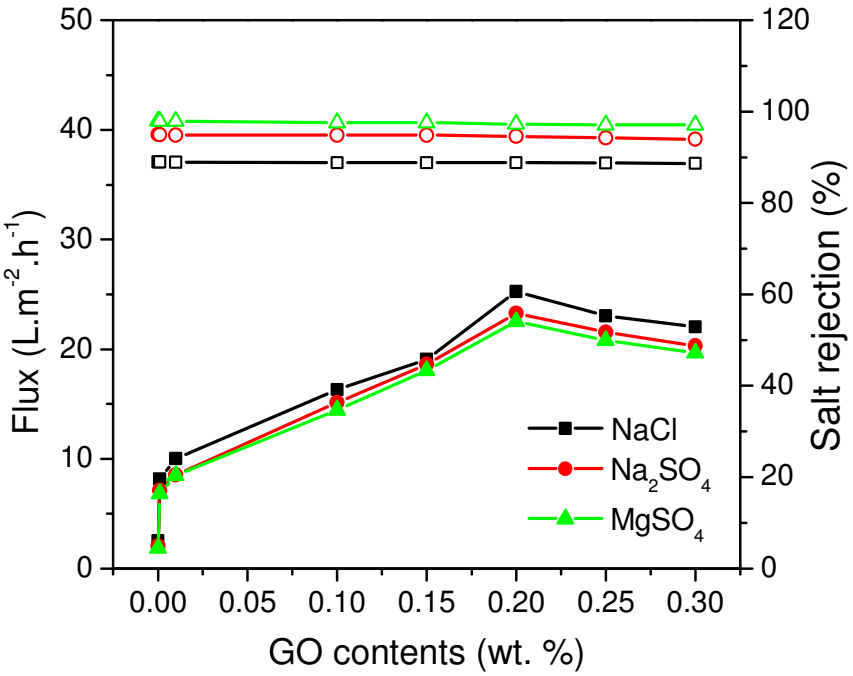

Figure 5 Permeation properties of PA membrane with different GO contents [NaCl, Na_2SO_4, $MgSO_4$ 2000ppm each]

The increase in water flux with increasing amount of GO could be attributed to various factors. The incorporation of GO improves the hydrophilicity of the membrane and thus contribute to an increase in water permeability. It is also known that the improved hydrophilicity of the membranes can enhance the water permeability by attracting water molecules inside the membrane matrix and facilitating them to pass through the membrane.[56] In addition to that, certain other factors may also be involved. First, the GO may provide an additional passageway for water molecules passing through. Second, the mobilization of GO disrupts polymer chain packing, leading to an increased system free volume. Third, some voids are unavoidably introduced into the thin-film layer at the GO/polymer interface by the incorporation of GO.[47, 54] However, the decrease in water flux caused by incorporating more than 0.2% GO might be caused by the aggregation of GO, at higher concentrations. The aggregation may lead to uneven distribution of GO in the thin-film layer, and similar results

were observed in other work with silica nanoparticles and ordered mesoporous carbon (OMC), [47–48] were due to the aggregation of filler, less water uptake and permeable flux were detected with higher loading of nanoparticles in the thin-film layer.

The effect of GO on permeation properties of polyamide membranes was also examined in terms of salt rejection. (Fig. 5) Three different salt solutions (of NaCl, $MgSO_4$, and Na_2SO_4) of (2,000 ppm) were used for this testing. With the increasing GO content, the flux of the salt solution increased, but with only a negligible change in the rejection properties of the membrane. The salt rejection of the PA membrane was 89% for NaCl and 98% for $MgSO_4$, while that of PA/GO was maintained above 88% and 97% for NaCl and $MgSO_4$, respectively. As expected, the salt rejection of the GO/PA membrane decreased as per the order $MgSO_4$ > Na_2SO_4 >NaCl. The better rejection of $MgSO_4$ than NaCl is likely due to the combined actions of electrostatic repulsion and size sieving effects.[49] The prepared membranes were negatively charged within the pH range of (6–10), and thus offered a stronger repulsive force to divalent SO_4^{2-} than to monovalent Cl^{1-}. Therefore, SO_4^{2-} ions face more resistance when penetrating the membrane. These results exhibit a sequence similar to the one reported previously for a negatively charged membrane. [50–51,55] Conversely, a small decrease in the salt rejection with increasing GO concentration, revealed that modification of the PA active layer with GO did not negatively affect the performance of the PA membrane. These results indicate that GO is a significant nanomaterial for modification of TFC membranes. Clearly, 0.2% GO should be considered the optimal GO concentration as the membrane prepared by adding this amount of GO exhibited the maximum flux. Further experiments were conducted in which additives were introduced into the MPD solution.[51]

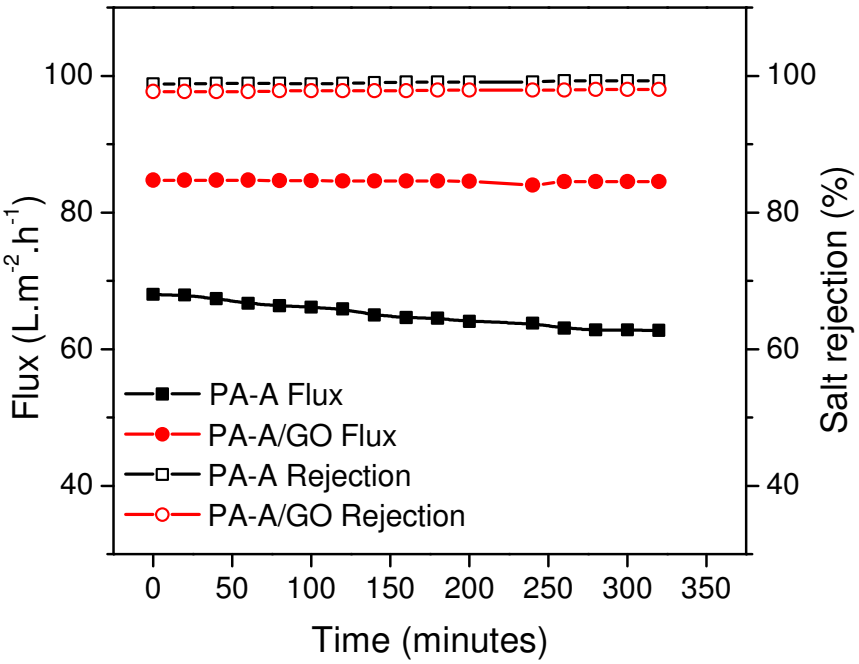

Figure 6 Permeation properties of PAA and PAA/GO (0.2%) membrane [$MgSO_4$ 2000ppm]

The addition of different additives in the aqueous phase has been attempt to improve the water flux of the TFC membrane without a significant loss of its salt-rejection capability.[51] Although, the use of additives can

influence the rate and extent of interfacial polymerization as well as the extent of cross linking, [52] it can simultaneously increase the susceptibility of the membrane to fouling. Polyamide membranes with additive (PA-A) were prepared with and without 0.2% GO (PA-A/GO), and their permeation characteristics were examined using a feed solution of 2,000 ppm $MgSO_4$. The PA-A membrane exhibited a higher flux value than the PA membrane, with no significant change in salt rejection. However, the flux of the PA-A membrane was further improved with the addition of 0.2% GO, as shown in Fig. 6.

It is widely accepted that the fouling behavior of a membrane is related to both surface morphology and to surface charge. To evaluate their fouling resistance, both PA-A and PA-A/GO membranes were subjected to permeation tests with aqueous solutions of a model protein (bovine serum albumin BSA at 200 ppm) and a mixture of humic acid and calcium chloride (200ppm-20 ppm) as shown in Fig. 7.

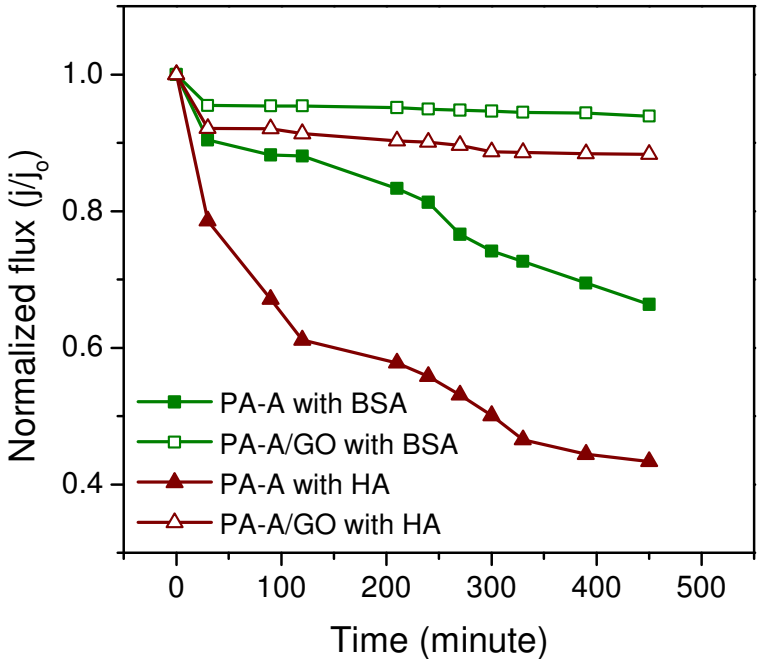

Figure 7 Characterization of PA-A and PA-A/GO membrane with humic acid (HA) and Bovine serum albumin (BSA)

In Fig. 7, the permeation trends for the PA-A and PA-A/GO membranes are compared as a function of time. The flux of PA-A/GO membranes slightly declined at first and then remained almost constant, while the PA-A membrane presented a continuous decrease in flux with time. Interestingly, the PA-A/GO membrane always maintained higher flux, which means that the performance of the membrane was significantly improved by the addition of GO. This suggests that the incorporation of GO improves the anti-fouling ability of membrane, which may be ascribed to the higher hydrophilicity that results from the hydrophilic groups of GO.[43] The surface adsorption properties of the membrane depend upon the hydrophilicity, thus improving the hydrophilicity of a membrane can reduce fouling to some extent. The hydrophilicity also helps to mitigate the adhesion of hydrophobic fouling materials to the membrane surface.[53] Model foulant such as BSA easily get adsorbed on hydrophobic surfaces to minimize the interfacial energy, but for surfaces with high hydrophilicity, this kind of adsorption does not offer any significant thermodynamic advantage. Therefore, this form of

fouling is inhibited. Thus, decreasing the hydrophobic character of the membrane by adding GO to introduce a more hydrophilic character, affects membrane performance dramatically.

Membrane roughness is another important parameter which affects fouling properties. Table 1 shows that the average surface roughness of the membrane decrease with the addition of GO. This is due to the reactions between the carboxyl groups of GO and TMC, which lead to decreased surface carboxylic groups. As a result, the effect of the divalent cation in humic acid solution can be reduced. Therefore, the addition of GO to a PA membrane not only increases its permeability, but also makes it stable against fouling.

Conclusions

A novel TFN membrane was prepared in the present study by interfacial polymerization, using an aqueous mixture of MPD-GO and organic TMC solutions on a polysulfone support. The GO loadings varied from (0 to 0.3) wt%. A better dispersion of GO occurred in the PA thin-film layer, as indicated by the ATR FT-IR results. With increasing concentration of GO, the hydrophilicity and zeta potential of the membranes, increased, and surface roughness decreased. The resultant increase in the permeate water flux was from (1.8 $L.m^{-2}h^{-1}$ to 22 $L.m^{-2}h^{-1}$) while salt rejection was maintained at essentially the same level (above 80%). The modified PA membranes exhibited excellent anti-fouling properties towards bovine serum albumin (BSA) and humic acid (HA). These results reveal that GO is a promising nano-material that could be used for the effective modification of commercial PA membranes at a relatively low cost.

AUTHOR INFORMATION

Corresponding Author

*Kew-Ho Lee

Email: khlee@krict.re.kr

Ph: +82 42 860 7240

Korea Research Institute of Chemical Technolgoy (KRICT), Gajeong-ro 141, Yuseong, Daejeon-South Korea

Author Contributions

The experimental work was performed by first author under the supervision of the corresponding author. The manuscript was written through the contributions of the first two authors. All authors have given approval to the final version of the manuscript.

ACKNOWLEDGMENT

The financial support for this project from Korea Research Institute of Chemical Technology (KRICT) is greatly acknowledged.

ABBREVIATIONS

NF, nanofiltration; PA, Polyamide; TFC, Thin film composite; TFN, thin film nanocomposite; PA-A,Polyamide with additives

REFERENCES

1. D. R. Dreyer, S. Park, C. W. Bielawski, R. S. Ruoff, *Chem Soc Rev*, 2010, **39**, 228.
2. D. A. Dikin, S. E. J. Stankovich, R.D. Zimney, G. H. B. Piner, Dommett, G. Evmenenko, S. T. Nguyen, R. S. Ruoff, *Nature*, 2007, **448**, 457.
3. M. Koinuma, C. Ogata, Y. Kamei, K. Hatakeyama, H. Tateishi, Y. Watanabe, T. Taniguchi, K. Gezuhara, S. Hayami, A. Funatsu, M. Sakata, Y. Kuwahara, S. Kurihara, Y. Matsumoto, *J. Phys. Chem. C*, 2012, **116**, 19822..
4. R. R. Nair, H. H. Wu, P.N. Jayaram, I. V. Grigorieva,A. K. Geim, *Science*, 2012, **335**, 442.
5. R. K. Joshi, P. Carbone, F. C. Wang, V. G. Kravets, Y. Su, I. V. Grigorieva, H. A. Wu, A. K. Geim, R. R. Nair, *Science*, 2014, **752**, 343.
6. T. M. Yeh, Z. Wang, D. Mahajan, B. S. Hsiao, B. Chu, J. Mater. Chem, DOI: 10.1039/c3ta12480k
7. D. P. Suhas, A. V. Raghu, H. M. Jeong, T. M. Aminabhavia, *RSC Adv*., 2013, **3**, 17120.
8. N. Wang, S. Ji, G. Zhang, J. Li, L. Wang, *Chem. Eng. J*, 2012, **213**, 318.
9. N. Wang, S. Ji, J. Li, R. Zhang, G. Zhang, *J. Membr. Sci*., 2014, **4551**, 113.
10. J. Lee, H. R. Chae, Y. J. Won, K. Lee, C. H. Lee, H. H. Lee, I. C. Kim, J. M. Lee, *J. Membr. Sci*., 2013, **448**, 223.
11. M. Hu, B. Mi, *Environ. Sci. Technol*., 2013, **47**, 3715.
12. F. Perreault, M. E. Tousley, M. Elimelech, *Environ. Sci. Technol. Lett*., 2013, 1, **71**.
13. B.M. Ganesh, A. M. Isloor, A.F. Ismail, *Desalination,* 2013, **313**, 199.
14. M. Elimelech, W. A. Phillip, Science , 2011, **333**, 712.
15. M. Hirose, Y. Minamizaki, Y. Kamiyama, *J. Membr. Sci*., 1997, **123**, 151.
16. Gu, J. E.; Jun, B. M.; Kwon, Y. N. *Water Res*., 2012, **46**, 5389.
17. D. H. Shin, N. Kim, Y. T. Lee, *J. Membr. Sci*., 2011, **376**, 302.
18. B. Mi, M. Elimelech, *Environ. Sci. Technol*., 2010, **44**, 2022.
19. B. Mi, M. Elimelech, *J. Membr. Sci*., 2010, **348**, 337.
20. D. L. Shaffer, N. Y. Yip, J. Gilron, M. Elimelech, *J. Membr. Sci*., 2012, **415**,1.
21. C. Liu, K. Rainwater,L. F. Song, *Desalination*, 2011, **276**, 352.
22. N.K. Saha, S.V. Joshi, *J. Membr. Sci*., 2009, **342**, 60.
23. V. Freger, J. Gilron, S. Belfer, *J. Membr. Sci*.,2002, **209**, 283.
24. S. Belfer, Y. Purinson, R. Fainshtein, Y. Radchenko, O. Kedem, *J. Membr. Sci*., 1998, **139**, 175.
25. S. Belfer, Y. Purinson, O. Kedem, *Acta Polym*.,1998, **49**, 574.
26. J. Gilron, S. Belfer, P. Väisänen, M. Nyström, *Desalination*, 2001, **140**, 167.

27. S. Yu, G. Yao, B. Dong, H. Zhu, X. Peng, J. Liu, M. Liu, C. Gao, *Sep. Purif. Technol*. 2013, **118** ,285.
28. J. Kim, B. Bruggen,. *Environ. Pollut*., 2010, **158**, 2335.
29. M. M. Pendergast, E. M. V. Hoek,. Energy and Environment Science, 2011, **4** , 1946.
30. S. Y. Lee, H. J. Kim, R. Patel, S. J. Im, J. H. Kim, B. R. Min, *Polym. Adv. Technol*. 2007,**18**, 562.
31. H. S.Lee, S. J. Kim, J. H. Kim, H. J. Kim, J. P. Kim, B. R. Min, *Desalination*, 2008, **219**, 48.
32. P. Aerts, S. Kuypers, I. Genne, R. Leysen, J. Mewis, I. F. J. Vankelecom, P.A. Jacobs, *J. Phys. Chem. B*, 2006, **110**, 7425.
33. B. J. Hinds, N. Chopra, T. Rantell, R. Andrews, V. Gavalas, L. G. Bachas, *Science*, 2004, **303** , 62.
34. B. H. Jeong, E. M. V. Hoek, Y. S.Yan, A. Subramani,X. F. Huang, G. Hurwitz,A. K. Ghosh, A. Jawor, *J. Membr. Sci*., 2007, **294** , 1.
35. J.S. Taurozzi, H. Arul, V. Z. Bosak, A. F. Burban, T. C. Voice, M. L. Bruening, V. V. Tarabara, *J. Membr. Sci.*,2008 , **325**, 58.
36. K. Zodrow, L. Brunet, S. Mahendra, D. Li, A. Zhang, Q. L. Li, P. J. J Alvarez , *Water Res*., 2009, **43**, 715.
37. S. R. Chae, S.Y. Wang, Z. D. Hendren, M. R. Wiesner, Y. Watanabe, C. K. Gunsch, *J. Membr. Sci*., 2009, **329**,68.
38. A. Tiraferri, C. D. Vecitis, M. Elimelech, *ACS Applied Materials and Interfaces*, 2011, **3** 2869.
39. L. Qiu, X. H. Zhang, W. R. Yang, Y. F. Wang, G. P. Simon, D. Li, *Chem. Commun*., 2011, **47**, 5810.
40. W.S. Hummers, R.E. Offeman, *J. Amer. Chem*. Soc.1958, **80**,1339.
41. N.I. Kovtyukhova, P.J. Ollivier, B.R. Martin, T.E. Mallouk, S.A. Chizhik, E.V. Buzaneva, A.D Gorchinskiy, *Chem. Mater*., 1999, **11**,771.
42. C. Zhao, X. Xu, J. Chen, F. Yang, *Journal of Environmental Chemical Engineering*, 2013, **1**, 349.
43. Z. Wang, H. Yu, J. Xia, F. Zhang, F. Li, Y. Xia, Y. Li, *Desalination*, 2012, **299**, 50.
44. N. K. Saha, S.V. Joshi, *J. Membr. Sci*, 2009, **342**, 60.
45. J. Zhang, Z. Xu, W. Mai, C. Min, B. Zhou, M. Shan, Y. Li, C. Yang, Z. Wang, X. Qian, *J. Mater. Chem. A* ,2013, **1**, 3101.
46. T. Szabó, E. Tombácz, E. Illés, I. Dékány, *Carbon*, 2006, **44**, 537.
47. J. Yin, E. S. Kim, J. Yang, B. Deng, *J. Membr. Sci*, 2012, **423–424** , 238.
48. E.-S. Kim, B. Deng, *J. Membr. Sci*. 2011, **375**, 46.
49. A. Santafe ´-Moros, J.M. Goza´lvez-Zafrilla, J. Lora-Garcı´a, *Desalination* , 2005, **185** 281.
50. M.Y. Kiriukhin, K.D. Collins, *Biophy. Chem*. 2002, **99**,155.
51. I.C. Kim, B.R. Jeong, S.J. Kim, K. H. Lee, *Desalination* ,2013, **308**, 111.
52. S.H. Kim, S.Y. Kwak, T. Suzuki, *Environ. Sci. Technol*.. 2005, **39**,1764.

53. L. L. Hwang, J. C. Chen, M. Y. Wey, *Desalination*, 2013, **313**,166.

54. H. Wu, B. Tang, P. Wu, *J. Membr. Sci*, 2013, **428**, 341.

55. H. Zhao; S. Qiu; L. Wu.; L. Zhanng, H. Chen, C. Gao.; *J. Membr. Sci*, 2014, **450** , 249

56. C. Zhao; X. Xu; J. Chen; F. Yang, *J.Environ. Chem. Eng*., 2013, **1**, 349

Graphic Abstract

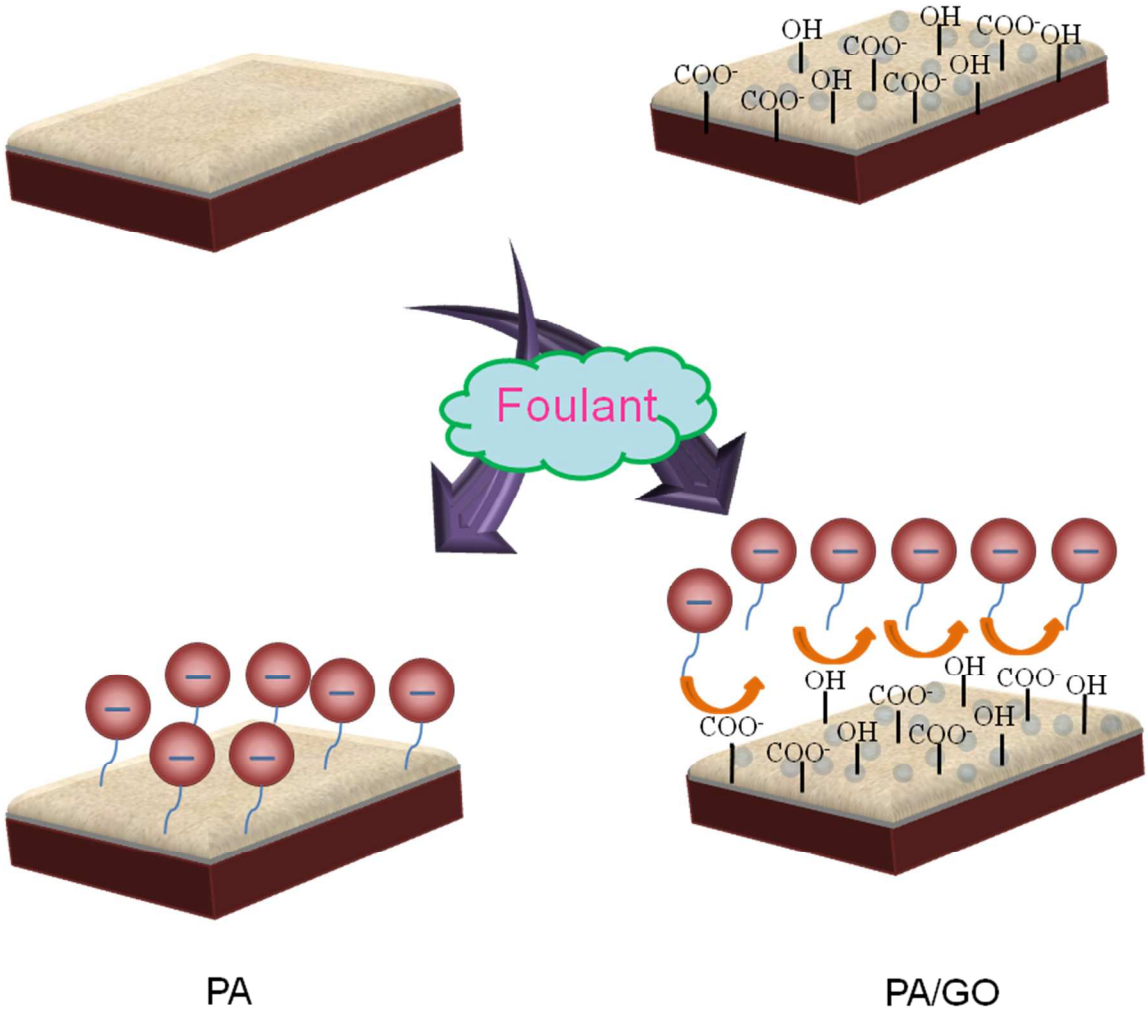

Conceptual visualization of GO effect on fouling